Photothermal transitions of magnetoexcitons in GaAs/$Al_xGa_{1-x}As$ quantum wells

J. Černe,[1] J. Kono,[2] M. Su,[3] and M. S. Sherwin[4]
[1]*Department of Physics, University at Buffalo, The State University of New York, Buffalo, New York 14260*
[2]*Department of Electrical and Computer Engineering, Rice University, Houston, Texas 77005*
[3]*National Institute of Standards and Technology 815.04, 325 Broadway, Boulder, Colorado 80305*
[4]*Department of Physics and Center for Terahertz Science and Technology, University of California, Santa Barbara, California 93106*
(Received 13 June 2002; published 1 November 2002)

By monitoring changes in excitonic photoluminescence (PL) that are induced by terahertz (THz) radiation, we observe resonant THz absorption by magnetoexcitons in GaAs/$Al_xGa_{1-x}As$ quantum wells. Changes in the PL spectrum are explored as a function of temperature and magnetic field, providing insight into the mechanisms which allow THz absorption to modulate PL. The strongest PL-quenching occurs at the heavy hole $1s \rightarrow 2p^+$ resonance where heavy hole excitons are photothermally converted into light hole excitons.

DOI: 10.1103/PhysRevB.66.205301 PACS number(s): 78.66.−w, 78.30.Fs, 71.35.Ji

Undoped quantum wells (QW's) have been studied extensively using interband optical techniques (for examples, see Ref. 1). These experiments have revealed a rich structure which is dominated by correlated electron-hole pairs known as excitons. Excitons in square QW form hydrogenlike states with binding energy of approximately 10 meV (the energy of a terahertz photon) and a Bohr radius on the order of 100 Å. The internal dynamics of excitons can be explored by using visible or near-infrared photons to create excitons, and THz radiation (of order 80 cm^{-1}, 10 meV, 2.4 THz) to manipulate them directly. At low THz intensities, one expects direct transitions between even- and odd-parity states of the exciton which are not observable with linear interband spectroscopy. Such transitions provide sensitive tests for the theory of excitons, which is fundamental in the physics of semiconductors. At higher THz intensities, one also can probe the dephasing and energy relaxation rates of excitons.[2]

Undoped direct gap (type I) QW's are especially interesting since they are so commonly used and provide a simple model system for theoretical analysis. However, the short lifetime of excitons in type I QW makes it difficult to achieve the large population of cold excitons required for conventional THz absorption studies. Experimental progress has been made in QW's using photoinduced absorption in staggered (type II) QW's (Ref. 3) and time-resolved THz spectroscopy in type I QW's.[4] Optically detected THz resonance (ODTR) spectroscopy was used to probe direct excitations of internal transitions of magnetoexcitons in type I QW's.[5,6] More recent work has included the study of charged[7–9] as well as neutral[10,11] magnetoexcitons in type I QW's.

Though ODTR has proven to be a powerful and successful technique, it remains an indirect measurement of THz absorption which still is not well understood. In this paper we use a multichannel technique to capture the full photoluminescence (PL) spectrum as a magnetic field sweeps exciton energy levels through THz resonances. We find a combination of resonant and quasithermal excitations are responsible for THz-induced changes in PL. In a particularly striking resonant process, THz radiation converts heavy-hole excitons to (radiative) light-hole excitons.

The undoped sample consists of fifty 100-Å-wide GaAs square QW's between 150-Å-wide $Al_{0.3}Ga_{0.7}As$ barriers.[12] The free-electron lasers (FEL) at the University of California, Santa Barbara, provide intense radiation (up to 1 MW/cm^2) that can be continuously tuned from 4 to 160 cm^{-1} (0.5–20 meV and 0.12–4.8 THz). As shown in Fig. 1, visible radiation from an Ar^+ laser is used to create electron-hole pairs in the undoped sample. Simultaneously, THz radiation with the electric field polarized in the plane of the QW, and therefore not coupling to intersubband transitions, passes through the sample. Measurements are performed with a visible laser excitation intensity of approximately 100 $W\,cm^{-2}$, creating an exciton density of approximately 3×10^{10} cm^{-2} per well in the sample.[13] The resulting PL is captured by 18 50-μm-diameter optic-fibers that surround a central fiber used for excitation. The PL is delivered to a monochromator and detected by an image-intensified charge-coupled device (ICCD) camera. The output of the Ar^+ laser is modulated acousto-optically to pro-

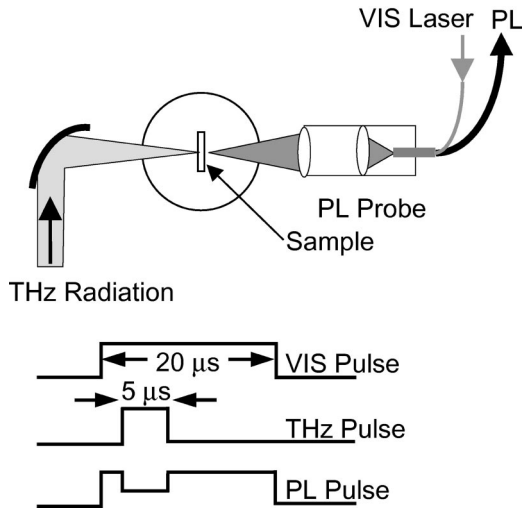

FIG. 1. A schematic of the experimental setup for MOTR measurements. Photoluminescence is detected while the THz pulse passes through the sample. The THz radiation is polarized parallel to the plane of the QW. The timing of the laser pulses and PL is shown in the lower half of the figure.

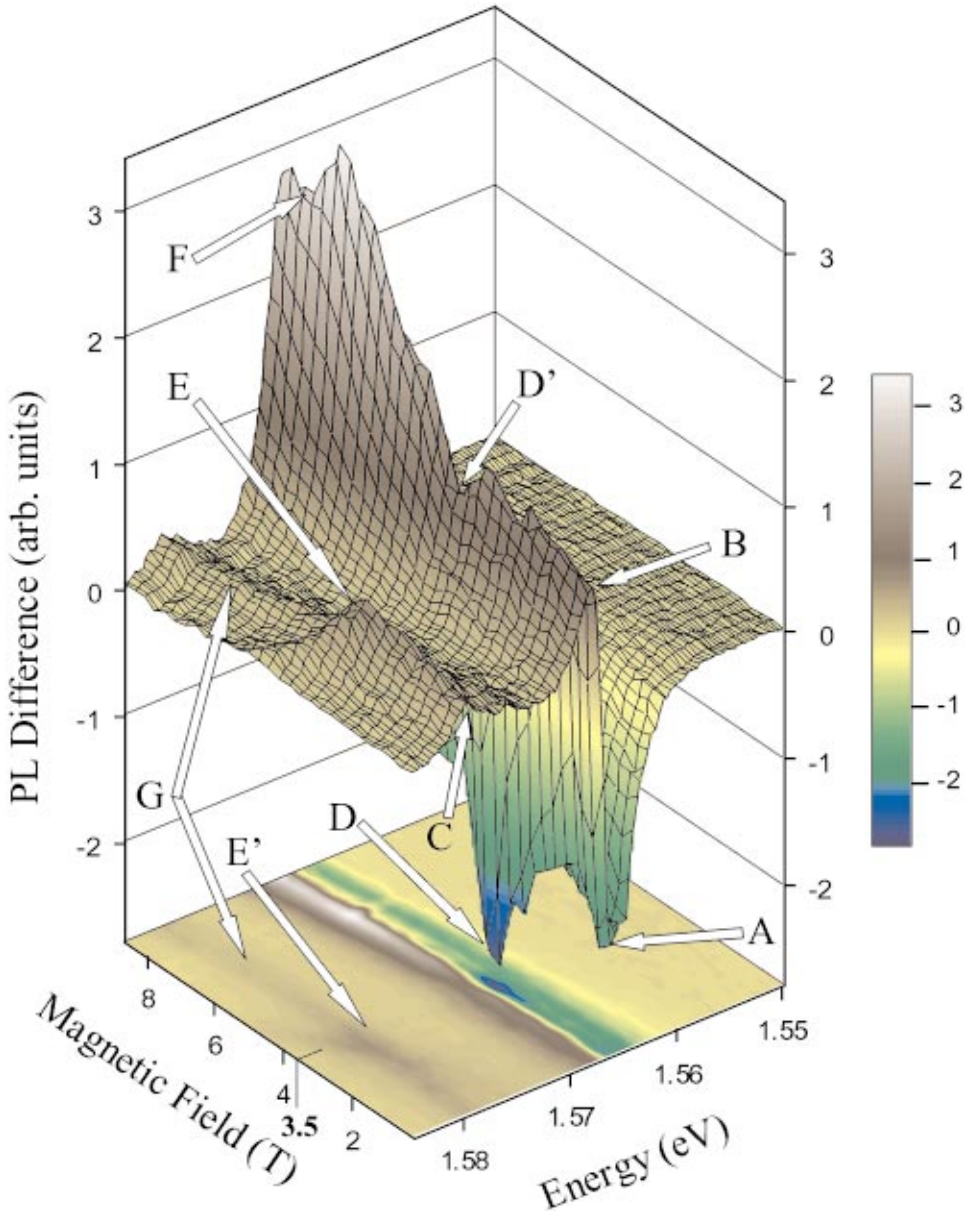

FIG. 2. (Color) PL spectra without THz irradiation subtracted from PL spectra with THz irradiation at 103 cm^{-1} as a function of *B*. The THz intensity is approximately 50 $kW\,cm^{-2}$. The sample temperature is 10 K.

duce a 20-μs visible excitation pulse that coincides with the 5-μs THz pulse at the sample. The repetition rate of the visible and THz radiation pulses is limited by the FEL repetition rate and is on the order of 1 Hz. The ICCD is gated in time to capture the entire PL spectrum while the THz radiation pulse illuminates the sample. Since the THz pulse is much longer than any carrier relaxation time, the measurement is in steady-state. The PL change during the THz pulse is due to carrier excitation; no lattice heating is observed.[14]

The measurement involves monitoring the PL spectrum as a function of the magnetic field *B* while fixed frequency THz radiation illuminates the sample. Unlike a single channel measurements using a photo-multiplier tube, the ICCD allows the entire PL spectrum to be captured at each value of *B*. This powerful technique is referred to as multichannel optically detected THz resonance (MOTR). A separate MOTR run is made with the THz radiation blocked to serve as a reference.

Figure 2 shows the difference of the PL spectra with and without THz irradiation plotted as a function of *B*. The THz frequency is 103 cm^{-1} and the intensity is approximately 50 kW/cm^2. The sample temperature is 10 K. Stronger PL quenching is represented by more negative values (shown in blue) of the PL difference. The false color image of this surface plot is projected on the bottom of the graph. There are strong qualitative differences in the PL modulation at different magnetic fields. Since experiments begin from $B=0$ T, it is convenient to label the excitonic states using a hydrogenic notation (principal quantum number, orbital angular momentum, z-projection of the orbital angular momentum). At $B=0$ T, the difference spectrum shows the quenching of the heavy hole $1s$ ($H1s$) PL peak amplitude (labeled

A in Fig. 2), the enhancement of high energy tail of the $H\,1s$ PL (B), and the enhancement of the light hole $1s$ ($L1s$) PL amplitude (C). These effects were previously observed and studied in detail.[14] As B increases, the $H1s$ PL amplitude is resonantly quenched at the $H1s \rightarrow H2p^+(m_z=+1)$ transition at 3.5 T (D and D'), while the $L1s$ PL reaches a maximum (E and E'). The THz-induced transitions from $H1s$ to $L1s$ states is clearly seen. At 8 T, further resonant quenching is observed (F) which is assigned to the $H2p^-(m_z=-1) \rightarrow H2s$ transition. Note that above 3.5 T, quenching is reduced and the dominant effect of THz radiation is to enhance and blueshift the $H1s$ PL peak (F). This can seen in the depth (height) of the PL difference surface plot above and below 3.5 T and is also shown by the color difference between these two regions in the projected image plot. A ridge that begins at 1.58 eV at 0 T and appears to follow the quadratic magnetic field dependence of the $H1s$ PL peak also is indicated (G). This ridge is consistently higher than the $H1s$ state by one THz photon energy throughout the magnetic field range. Note that this ridge appears to cross a more strongly curved second ridge at point E', which is where the $L1s$ is resonantly enhanced. Neither ridge is consistent with magnetic field dependence of PL from the $L1s$. Also note that the line where the PL difference sheet crosses zero (yellow line in the projected image plot) is nearly independent of magnetic field and does not follow the B^2 dependence of $H1s$ PL peak energy.

The information contained in Fig. 2 is more accessible when cross sections through this surface plot are examined. The resonant enhancement of the $L1s$ PL peak at the expense of the $H1s$ PL amplitude is shown in Fig. 3(b), where the $H1s$ and $L1s$ PL amplitudes are plotted against B. Note that this figure shows the PL amplitudes, not the normalized PL ratios (i.e., PL with divided by PL without THz irradiation, as shown in most ODTR spectra), which adds a baseline that depends on B. The $H1s \rightarrow H3p$ feature at 2.1 T splits into two dips ($H1s \rightarrow H3p^+$ and $H1s \rightarrow H3p^-$) above 2.5 T.[5,6,15] The $L1s$ PL enhancement is asymmetric in B, with a fast decay above 3.5 T, and a more gradual decrease below 3.5 T. The $H1s$ amplitude shows similar asymmetry and reflects the conventional ODTR results.[5,6] Figure 3(a) sketches the energy difference between the $H1s$ and higher energy exciton states (based on data published in Ref. 5). The diagrams in the inset of Fig. 3(a) sketch the photothermal carrier distributions at different magnetic fields, and will be discussed in greater detail later in this paper.

Absorption of THz radiation can heat carriers, resulting in a quasithermal distribution with a temperature above that of the lattice.[14] It is thus useful to compare changes in photoluminescence induced by THz radiation to those induced by changing the temperature of the sample. Figure 4 plots the $L1s$ to $H1s$ PL amplitude ratio as a function of inverse lattice temperature, without (a) and with (b) a THz irradiation of approximately 100 W cm^{-2}. These data form Arrhenius plots where straight lines indicate thermally activated population of the $L1s$ from $H1s$ states. The slopes of these lines determine the activation energies E_A, which are shown in the

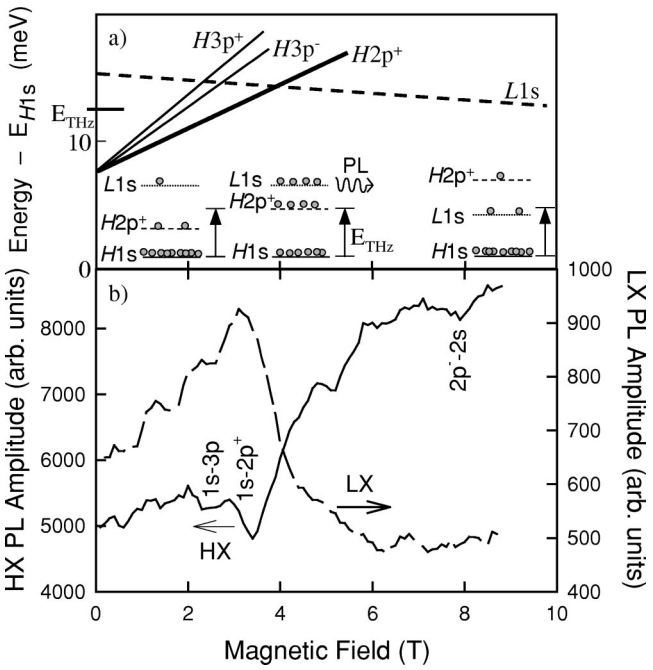

FIG. 3. Energies relative to the $H1s$ state of higher energy excitonic states are schematically shown in (a). Solid lines indicate energy levels (e.g., $H2p^+$) that are accessible from the $H1s$ state via radiative transitions. When $B=B_{1s-2p^+}$, the THz photon energy matches the $H1s \rightarrow H2p^+$ energy separation. Note that for $B > 3.5$ T, the $H2p^+$ state is above the $L1s$ state. Inset in (a) are simple representations of the thermal and photothermal carrier distributions induced by THz irradiation. The $L1s$ and $H1s$ PL amplitudes are plotted as a function of B under THz illumination at 10 K in (b). These data are obtained from cross-sectional slices that follow the $L1s$ and $H1s$ PL energies in Fig. 2.

legends of Fig. 4. Note the dramatic decrease in the activation energy when the sample is illuminated by THz radiation at 3.5 T.

We propose a qualitative explanation of THz-induced changes in PL which involves three processes. (1) Absorption: THz radiation is absorbed via internal transitions of excitons,[5,6,15,7,11] or by Drude-like free carrier excitations of ionized electrons and holes.[14] (2) Quasithermalization: Each species of excitons (for example, $H1s$, $H2p^+$, or $L1s$), is associated with a band of states with different center-of-mass momenta. The power transferred into the electron-hole system indirectly heats each band of excitons to a temperature warmer than that of the lattice. (3) Luminescence: The luminescence under THz irradiation only reflects the population of states that can participate in radiative interband transitions. In bands with even parity ($1s$ and $2s$, for example), the radiative states are those with an in-plane momentum K_{COM} near zero. In bands with odd parity, such as $2p$, no states are radiative.

We now discuss the experimental data as a function of increasing magnetic field with a fixed THz frequency of 103 cm^{-1}. The case $B=0$ T has been studied extensively in Ref. 14. In this nonresonant case, the mechanism for absorption was shown to be a Drude-like heating of ionized electrons and holes. These hot electrons and holes heat luminesc-

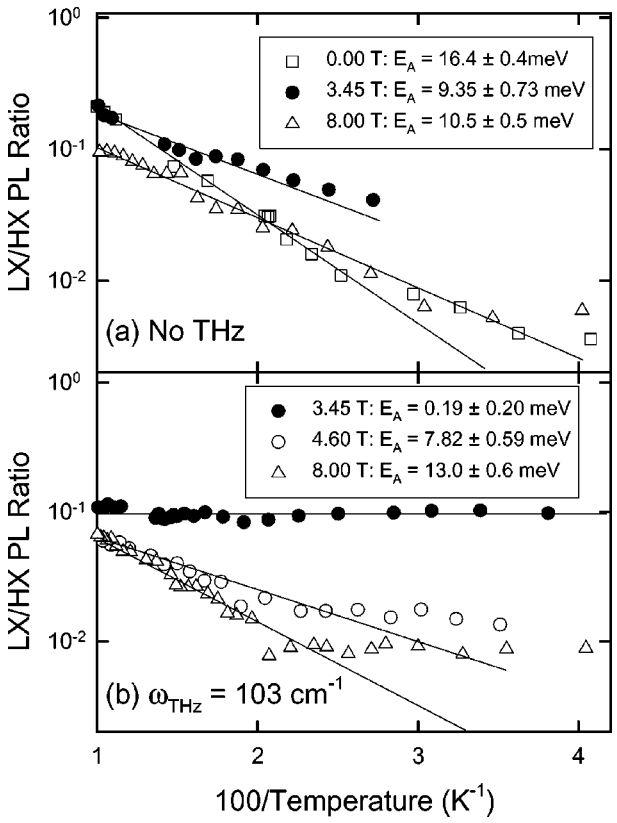

FIG. 4. Arrhenius plot of the $L1s/H1s$ ratio without (a) and with (b) THz irradiation. The THz intensity is approximately 100 kW cm^{-2}. The straight lines represent activated behavior with an activation energy that is determined by the slope of the line. Activation energies that are obtained from exponential fits are shown in the legends. The $L1s$-$H1s$ energy spacing measured from PL is approximately 14 meV for all B. The $H2p^+$-$L1s$ separation is approximately 1 meV at 3.45 T.

ing excitons. The nonresonant photothermal distribution is represented by the cartoon on the left side of the inset in Fig. 4(a). Under THz illumination, the exciton system (including both $H1s$ and $L1s$ excitons) could be reasonably well described by a single temperature larger than that of the lattice. This temperature could be measured by matching the PL spectrum with THz irradiation at a low lattice temperature to the PL spectrum without THz radiation at an elevated lattice temperature. As either temperature or THz power increases, the magnitude of $H1s$ luminescence decreases, and the $L1s/H1s$ PL ratio increases. Either of these quantities could be used to measure the temperature of the exciton system. Both measures produce consistent results.[14]

Between 0 T and about 3.5 T, the qualitative features of Figs. 2 and 3 are similar to those at $B=0$, with a quenching of the $H1s$ luminescence and enhancement of $L1s$. In this regime, there are many internal states which have energies below that of the 103-cm^{-1} pump, and which can be excited by it.

One of the most striking features of the data is the resonant transfer of PL from $H1s$ to $L1s$ which occurs near 3.45 T (E and E' in Fig. 2; also see Fig. 3). Our explanation is a resonant photothermal mechanism, shown schematically in the central cartoon in the inset of Fig. 3(a). THz radiation promotes excitons from $H1s$ to $H2p^+$. The dark $H2p^+$ state[16] is only about 1 meV below the radiative $L1s$ state according to PL and ODTR data. Thermal fluctuations, associated with the quasitemperature of the $H2p^+$ excitons, are sufficient to then populate $L1s$ exciton states to a much greater degree than they could be populated via thermal excitation directly from $H1s$. According to photothermal ionization experiments on shallow donors in GaAs,[17] the $2p^+$ state allows extremely efficient ionization. Reference 17 found that the probability of ionization from the $2p$ state is much larger than expected from the energy separating this state and the continuum; the ionization probability at 4.2 K is essentially unity.[18] $L1s$ excitons decay, emitting the observed luminescence. The photo-thermal hypothesis is supported by the observation that, in Fig. 4(b), the ratio of $L1s$ to $H1s$ luminescence is nearly independent of temperature for the case of THz on, $B=3.45$ T. This demonstrates an effective activation energy which is negligible. In contrast, without THz irradiation, the $L1s/H1s$ at 3.45 T increases strongly with temperature, consistent with an activation energy on the order of 10 meV.

A second hypothesis is that the THz radiation heats the entire exciton system efficiently on resonance, but that all bands of excitons can still be described with a single temperature. We call this the thermal hypothesis. The thermal hypothesis could be consistent with the insensitivity of the $L1s/H1s$ ratio to increasing temperature at resonance. However, it predicts that, as was observed for $B=0$ T, the photoluminescence spectrum under THz illumination at low temperatures can be mapped onto the photoluminescence spectrum without THz excitation at some higher temperature. This is not the case. At 3.45 T and at a lattice temperature of 10 K with THz illumination of 110 kW/cm^2, the $H1s$ PL amplitude is the same as for a lattice temperature of 70 K without THz illumination at 3.45 T. However, the $L1s$ peak for the cold sample illuminated with THz is over 40% larger than for the unilluminated warm sample. Furthermore, the $L1s$ PL amplitude increases linearly with THz intensity at the $H1s \rightarrow H2p^+$ resonance, while the increase in the absence of THz illumination is consistent with exponentially activated behavior as a function of temperature. This is consistent with the photothermal hypothesis, and inconsistent with the thermal hypothesis.

Above 3.45 T, the changes in photoluminescence induced by THz irradiation are qualitatively different from those induced at lower magnetic fields. At high magnetic fields in Fig. 3(a), the THz photon energy is smaller than the lowest dominant exciton transition ($H1s \rightarrow H2p^+$). The high magnetic field photothermal distribution is shown schematically in the cartoon on the right side of the inset in Fig. 3(a). In this regime, lower energy exciton transitions (e.g., $H2p^- \rightarrow H2s$) can occur, and the hot carriers can impact with and heat cold excitons, which produces a PL quenching signal at 8 T in Fig. 2. The heating is not efficient and high THz, and visible intensities are required to produce the $H2p^- \rightarrow H2s$ feature. There are several reasons for this reduced efficiency. First, at low temperature, most of the carriers are bound in $1s$ (ground state) excitons, so the population in excited states

(e.g., $2p^-$ which has an energy that has a characteristic temperature of 80 K above the $1s$ state), especially at low THz and visible intensities, is significantly lower than the $1s$ population. Higher intensities increase the exciton temperature, and hence enhance the population of $2p^-$ excitons that can participate in the $H2p^- \rightarrow H2s$ transition. Second, PL amplitudes are not as sensitive to temperature changes at higher B. Finally, most hot heavy hole excitons (HX's) (with center of mass momentum $K_{\mathrm{COM}} \neq 0$) will eventually cool to contribute to the main HX PL line within the radiative cone ($K_{\mathrm{COM}} \approx 0$). Since radiative recombination for the hot HX's ($K_{\mathrm{COM}} \neq 0$) is suppressed due to momentum conservation, and since nonradiative recombination is weak, most of the hotter HX's have nowhere to go but back to the $K_{\mathrm{COM}}=0$ state where they can efficiently recombine radiatively. The closest escape for HX's is the $L1s$ which is over 14 meV (163 K) higher in energy at $B=0$ [see Fig. 3(a)]. This activated behavior can be seen in Fig. 4, where the activation energy to populate the $L1s$ state is approximately 10 meV without (a) and with (b) THz irradiation at 8 T. As a result, heating may increase the $H1s$ lifetime as it journeys through K_{COM} space, but will not significantly change the quantum efficiency of the $H1s$ PL nor the steady-state ODTR signal.

This model does not explain the THz-induced enhancement and blueshift of the $H1s$ PL amplitude. One expects an energy shift in the PL close to THz resonances due to the ac Stark effect.[19] The calculated shift changes sign depending on whether the THz pump frequency is higher or lower than the transition frequency. One would expect an intensity-dependent blueshift (redshift) in the exciton absorption spectrum when the driving photon energy is above (below) the unperturbed transition energy. The data, on the other hand, show a shift that increases monotonically with B. The apparent lack of a Stark shift may be due to the fact that excitonic transition energies are swept across the energy of the photons in the strong THz radiation field. As a result the difference between the transition frequency and the pump frequency (detuning frequency) is not fixed, but is swept continuously from positive to negative values, and hence no single laser induced energy shift is observed. This may in fact lead to a broadening of the absorption due to the transition energy shifting as the detuning energy is swept through zero. Furthermore, since the THz radiation is both the pump and probe, it is more difficult to isolate THz-induced shifts in the exciton transition energy.

MOTR has been used to study the THz dynamics of magnetoexcitons in GaAs QW's. Excitonic transitions have been identified and are in good agreement with theory. A simple qualitative model can be used to understand the PL modulation due to THz radiation. On the other hand, this work has generated several new puzzles which still require exploration. The MOTR baseline and the higher energy ridge (labeled G in Fig. 2) that follows the $H1s$ peak are still not clearly understood. The higher energy ridges (G and E' in Fig. 2) appear to indicate mixing of excitonic and photonic states. Significant energy shifts of over 3 meV are observed in the $H1s$ PL close to $H2p^- \rightarrow H2s$, which may be related to an ac Stark effect. The information gained from studying excitons in QW will provide an important foundation for research of excitons in even lower dimensional systems such as quantum wires and dots.

The authors gratefully acknowledge the assistance of T. Gutierrez, G.E.W. Bauer, and A.B. Dzyubenko. Samples were kindly provided by M. Sundaram and A. C. Gossard. We would also like to thank D.P. Enyeart and J.R. Allen at the Center for Terahertz Science and Technology for their technical support. This work was supported by the NSF Science and Technology Center for Quantized Electronic Structures DMR 91-20007, NSF-DMR 0070083, ONR N00014-K-0692, AFOSR 88-0099, and the Alfred P. Sloan Foundation (MSS). All measurements were performed at the Center for Terahertz Science and Technology, University of California, Santa Barbara, California.

[1] *The Spectroscopy of Semiconductors*, Semiconductors and Semimetals, Vol. 36, edited by D.G. Seiler and D.L. Littler (Academic Press, New York, 1992).

[2] For examples, see J.N. Heyman, K. Unterrainer, K. Craig, B. Galdrikian, M.S. Sherwin, K. Campman, P.F. Hopkins, and A.C. Gossard, Phys. Rev. Lett. **74**, 2682 (1995); H. Schwab, V.G. Lysenko, J.M. Hvam, M. Urban, and C. Klingshirn, J. Cryst. Growth **117**, 778 (1992); T. Dekorsy, R. Ott, P. Leisching, H.J. Bakker, C. Waschke, H.G. Roskos, H. Kurz, and K. Kohler, Surf. Sci. Spectra **40**, 551 (1996).

[3] C.C. Hodge, C.C. Phillips, M.S. Skolnick, G.W. Smith, C.R. Whitehouse, P. Dawson, and C.T. Foxon, Phys. Rev. B **41**, 12319 (1990).

[4] R.H.M. Groeneveld and D. Grischkowsky, J. Opt. Soc. Am. **11**, 2502 (1994).

[5] J. Černe, J. Kono, M.S. Sherwin, M. Sundaram, A.C. Gossard, and G.E.W. Bauer, Phys. Rev. Lett. **77**, 1131 (1996).

[6] M.S. Salib, H.A. Nickel, G.S. Herold, A. Petrou, B.D. McCombe, R. Chen, K.K. Bajaj, and W. Schaff, Phys. Rev. Lett. **77**, 1135 (1996).

[7] H.A. Nickel, G.S. Herold, T. Yeo, G. Kioseoglou, Z.X. Jiang, B.D. McCombe, A. Petrou, D. Broido, and W. Schaff, Phys. Status Solidi B **210**, 341 (1999).

[8] A.B. Dzyubenko, A.Y. Sivachenko, H.A. Nickel, T.M. Yeo, G. Kioseoglou, B.D. McCombe, and A. Petrou, Photonics Spectra **6**, 156 (2000).

[9] G. Kioseoglou, H.D. Cheong, T. Yeo, H.A. Nickel, A. Petrou, B.D. McCombe, A.Y. Sivachenko, A.B. Dzyubenko, and W. Schaff, Phys. Rev. B **61**, 5556 (2000).

[10] H.A. Nickel, G. Kioseoglou, T. Yeo, H.D. Cheong, A. Petrou, B.D. McCombe, D. Broido, K.K. Bajaj, and R.A. Lewis, Phys. Rev. B **62**, 2773 (2000).

[11] G.S. Herold, H.A. Nickel, J.G. Tischler, B.A. Weinstein, and B.D. McCombe, Physica E **2**, 39 (1998).

[12] S.M. Quinlan, A. Nikroo, M.S. Sherwin, M. Sundaram, and A.C. Gossard, Phys. Rev. B **45**, 9428 (1992).

[13] The exciton density is determined using the absorption coefficient for GaAs at 532 nm of 8×10^4 cm^{-1} and an exciton lifetime of 0.5 ns.

[14] J. Černe, A.G. Markelz, M.S. Sherwin, S.J. Allen, M. Sundaram, A.C. Gossard, P.C. van Son, and D. Bimberg, Phys. Rev. B **51**, 5253 (1995).

[15] H.A. Nickel, G. Kioseoglou, T. Yeo, H.D. Cheong, A. Petrou, B.D. McCombe, D. Broido, K.K. Bajaj, and R.A. Lewis, Phys. Rev. B **62**, 2773 (2000).

[16] Single photon radiative recombination is forbidden for the $2p^+$ state, and nonradiative recombination is also weak.

[17] G.E. Stillman, C.M. Wolfe, and D.M. Korn, Lincoln Lab. Massachusetts Inst. Technol., Lexington, Mass. in *Proceedings of the International Conference on the Physics of Semiconductors, Warsaw, Poland, 1972*, Meeting Date 1972, 2 863-9. (PWN-Pol. Sci. Publ., Warsaw), 291AAX, Conference written in english.

[18] Above approximately 3 T, the $H2p^+$ is in fact higher in energy than the HX continuum.

[19] For references discussing the THz Stark effect in semiconductor quantum heterostructures see B. Birnir, B. Galdrikian, R. Grauer, and M. Sherwin, Phys. Rev. B **47**, 6795 (1993); M.S. Sherwin, in *Quantum Chaos*, edited by G. Casati and B.V. Chirikov (Cambridge University Press, Cambridge, 1998), p. 209; K.B. Nordstrom, K. Johnsen, S.J. Allen, A.-P. Jauho, B. Birnir, J. Kono, T. Noda, H. Akiyama, and H. Sakaki, Phys. Rev. Lett. **81**, 457 (1998).